Research Article

Chern Yang Leong, Seong Shan Yap*, Guang Liang Ong, Teng Sian Ong, Seong Ling Yap, Yoong Tatt Chin, Siaw Foon Lee, Teck Yong Tou, and Chen Hon Nee*

Single pulse laser removal of indium tin oxide film on glass and polyethylene terephthalate by nanosecond and femtosecond laser

https://doi.org/10.1515/ntrev-2020-0115
received December 8, 2020; accepted December 22, 2020

Abstract: Indium tin oxide (ITO) is the most important transparent conducting electrode to date and the candidate for ultrafast signal processing in telecommunication region. ITO is normally selectively removed in a multiple-steps process for device application. In this work, we aimed to study single pulse removal of ITO-coated glass and PET by using a nanosecond (ns) laser (266 nm) and a femtosecond (fs) laser (1,025 nm) where each process is dominated by either linear or nonlinear process. For ns laser, ITO was removed from PET substrate at 0.01 J/cm^2. Detachment likely occurred via thermal-induced process because of the high absorption by both ITO and PET and the thermomechanical properties of PET. At higher laser fluence (~0.04 J/cm^2), the ITO films on both substrates were damaged, and at 1.34 J/cm^2, ITO was ablated from the glass substrate. For fs laser removal via nonlinear process, ITO was removed from PET substrate at 0.3 J/cm^2, but at 0.8 J/cm^2, the PET substrate was also modified. ITO layer was partially removed from glass substrate by fs laser pulse at 0.3 J/cm^2 and full removal only occurred at 1.7 J/cm^2. Thus, the fluence range for single fs pulse removal of ITO/PET was 0.3–0.8 J/cm^2 and >1.7 J/cm^2 for ITO/glass.

Keywords: ITO, laser processing, transparent conducting oxide

1 Introduction

Tin-doped indium oxide or indium tin oxide (ITO) is the most important transparent conductive oxide (TCO) as transparent electrodes due to their excellent electrical conductivity and optical transparency in the visible spectrum [1,2]. It is used in almost all optoelectronic applications such as displays, touch panels, solar cells, and sensors [3,4]. In the recent years, ITO is also gaining importance in the area of nanophotonics [5] as it is discovered to possess large optical nonlinearity in the epsilon-near-zero (ENZ) region [6,7]. The region coincides with the near infrared (NIR)/telecommunication wavelength, leading to potential applications in ultrafast switching applications for all optical computing [8,9]. In addition to the distinct properties, it is also compatible with complementary metal oxide semiconductor (CMOS) fabrication technology. The variety of applications requires ITO-coated substrate to be removed, patterned, or forming isolated electrodes with the desired shape. Selective removal of ITO is done using lithography or wet etching technique. Special mask is required for each design and the process involves multiple steps. Thus, the ability to pattern it at ease will enable the use in new device architecture and design. Another approach for ITO patterning is to utilize lasers in a dry process which offers higher controllability, potentially negating the necessity of masking, thus reducing the complexity of patterning process [10–15].

Lasers have been used in various materials or device fabrication process: synthesis, deposition, micromachining, etching/patterning, annealing, and fusing because of the clean coherent photons as energy source [16]. Pulsed lasers

* **Corresponding author: Seong Shan Yap,** Faculty of Engineering, Multimedia University, Jalan Multimedia, 63100, Cyberjaya, Selangor, Malaysia, e-mail: seongshan@gmail.com
* **Corresponding author: Chen Hon Nee,** Faculty of Engineering, Multimedia University, Jalan Multimedia, 63100, Cyberjaya, Selangor, Malaysia, e-mail: neechenhon@gmail.com
Chern Yang Leong, Guang Liang Ong, Teng Sian Ong, Teck Yong Tou : Faculty of Engineering, Multimedia University, Jalan Multimedia, 63100, Cyberjaya, Selangor, Malaysia
Seong Ling Yap: Plasma Technology Research Centre, Department of Physics, Faculty of Science, University of Malaya, 50603, Kuala Lumpur, Malaysia
Yoong Tatt Chin: SanDisk Storage Malaysia Sdn, Bhd, Batu Kawan, 14100, Penang, Malaysia
Siaw Foon Lee: Spanish National Research Council, Eduardo Torroja Institute for Construction Science (IETcc-CSIC), Madrid, Spain

are especially useful for removal or patterning without using any mask as the instantaneous pulse energy is localized within a short duration of time. The laser-materials interaction mechanisms by fs pulse laser are distinctly different than those operated at ns timescale [17]. When ultrafast laser is used, the timescale of laser-material interaction can be even shorter than the lattice vibration time and that there is insignificant or no heat diffusion away from the interaction area. As a result, the heat-affected zone or melting is minimized [18]. In addition, ultrafast laser also enables the processing of transparent materials because of nonlinear absorption mechanisms [19,20]. Such ultrashort pulse may offer a solution to not just micro and nanofabrication, but also for patterning or removal of wide bandgap materials [21,22].

In early years, the laser removal of ITO was performed by using ns laser. The use of ns laser at 262, 349, 523, and 1,047 nm has shown different removal efficiencies for ITO (150 nm) [23]. The line scanned by the 262 nm laser with spatial overlap of about 40% between the successive pulses at 3 J/cm^2 was clean, while the infrared laser (1,047 nm) at 18 J/cm^2 created line with residue. The results are attributed to the absorption and heating of the glass substrate at different wavelengths. The threshold was substantially lower (0.83–2.38 J/cm^2) for thin ITO layer (30 nm) by ns laser pulse (226, 355, 532, and 1,064 nm) [24]. In both studies, the threshold was lower in ultraviolet range than visible and at NIR. When an ultrafast laser pulse with picosecond (ps) and fs pulse width is used, the ablation characteristics and mechanisms are different [25–27]. In a study of 10 and 150 ps IR laser ablation of ITO (175 nm) on glass substrate, it was found that thermal ablation occurs for 150 ps laser and stress-assisted ablation is responsible for the ablation by 15 ps laser in multiple pulse experiment [28]. For ultrafast laser ablation of ITO, the fluence range was lower than ns laser (~0.25–0.32 J/cm^2) and there were no clear dependence on laser wavelength. In another work, 150 fs pulse (775 nm) was used, the ablation threshold of ITO (150 nm) was ~0.7–0.82 J/cm^2, but a complete removal required 1.2 J/cm^2 [29]. Although the threshold for ablation is low, a complete removal of ITO normally requires multiple laser pulse scanning across the ITO layer [30]. It was also suggested that incubation effects by the high frequency laser pulse lowered the ITO ablation thresholds. In order to obtain good resolution in the ablation depth, ablation from a square and flat top fs laser was studied [31]. Upon multiple exposures, the square-shape ablation depth of 40–150 nm can be obtained.

ITO coated on polyethylene terephthalate (PET) enables flexible electronics such as sensors, solar cells [3], display, and wearables [32]. However, the use of pulsed laser for removal of ITO on PET or polymers has not been explored extensively as compared to ITO on glass. Patterning of ITO on PET substrate is more challenging as compared to glass substrate as PET has lower resistance to chemical and less resilient to heat as compared to glass. Thus, the threshold fluence for ablation of ITO on PET substrates should be controlled and limited to avoid any damage to the PET substrate. Among the few reports on laser removal of ITO on PET, the results vary. For example, 10 μm ITO line was successfully removed without substrate damaging by 248 nm laser patterning of ITO on PET [33]. However, in another study, 266, 355, 532, and 1,064 nm laser were used for removal of very thin ITO films (30 nm) on PET substrates and severe damage to the PET substrate was observed by 266 nm [34]. Alternatively, a pre-patterned metal film was tested as the dynamic release layer in indirect laser patterning of ITO for pentacene thin film transistor [12]. When 355 nm laser with picosecond pulse was used to remove 130 nm thick ITO at 0.05 J/cm^2, roughening of the barrier layer beneath the surface was observed above 0.075 J/cm^2 [13]. The results indicate that precise control in laser energy, pulse width, frequency, and overlapping rate between successive spots at different laser wavelengths is required to remove ITO films and at the same time avoid substrate damage [13,33,35].

In the current work, we intend to systematically study and compare single pulse removal of ITO from both glass and PET substrates. The thickness of the ITO used is 110–120 nm, which are typically used in various devices. Two types of lasers are used; a ns laser (266 nm) and a fs laser (1,025 nm). Significant thermal absorption of ITO is anticipated in the case of 266 nm laser, and low or insignificant thermal process is expected when a fs laser is used. Single fs laser pulse interaction with ITO and the substrates is of interest for its potential to be used in prototyping and advanced fabrication processes. Transparent substrates can be micromachined [19] and therefore can be damaged by the ultrafast laser pulses; thus the process has to be controlled carefully to avoid such damage. The thresholds for ablation/damage, complete removal as well as substrate damage are studied. The removal mechanisms and the nonlinear or multiphoton absorption process involved are investigated. A comparison is made with the reported works that have laid the foundation on the topic of study.

2 Experimental

Commercially available ITO-coated glass (ITO/glass) and ITO-coated PET film (ITO/PET) (639303, Sigma-Aldrich, 127 μm) are used in this work. The thickness of the ITO coating on glass substrate is 110 nm, while the thickness for ITO on PET film is 120 nm, measured by profilometer (Mahr). The sheet resistance of ITO coating on glass is 15 Ω/sq and ITO on PET is 60 Ω/sq. The transmittance of the ITO samples is measured by using a deuterium halogen light source and spectrometer (Avantes) and the sheet resistance is measured by 4 point probe method (Keithley). A ns pulsed Nd:YAG laser with 4th harmonic (266 nm, 8 ns, Lotis TII) and a fs pulsed laser (1,025 nm, 500 fs, Amplitude Systemes) are used for laser patterning. The laser beam is directed onto the sample placed on a moving stage through a series of mirrors, aperture, and lenses. The maximum laser energy for ns laser is 6 mJ and the maximum laser energy for fs laser is 650 μJ. The fluence of the laser can be controlled by controlling the focused beam size. For ns laser, the laser energy is varied from 45 μJ to 6 mJ and the sample moves at speed ranging from 500 mm/min to 1,000 mm/min. The laser repetition rate is fixed to 10 Hz. For the fs laser, the laser energy is varied from 61 to 620 μJ. The speed of the sample stage is controlled in order to achieve the desired overlapping of laser beams between each successive spot. Prior to laser ablation, the sample is covered with a thin layer of isopropyl alcohol. The laser energy is measured by an energy meter (Ophir) and the samples are inspected by using microscopes (magnification up to 500×, Nikon ME600), atomic force microscope (tapping mode, Nanosurf) after laser patterning.

3 Results and discussion

The transmittance of the sample ITO on glass, taken with reference to the glass substrate, and the transmittance of ITO on PET with reference to the PET substrate are shown in Figure 1a. The transmittances of the substrates are shown in Figure 1b. Both ITO and the substrate (glass/PET) are not transmitting at 266 nm. At 1,024 nm, ITO film on PET has lower transmission than the ITO film on glass. Commercial ITO on glass possesses higher transmittance as they are typically deposited by sputtering with substrate heating. The transmittance of the substrate of 1 mm glass and 127 μm thick PET is about the same at 266 nm (~0%) and 1,024 nm (~86%).

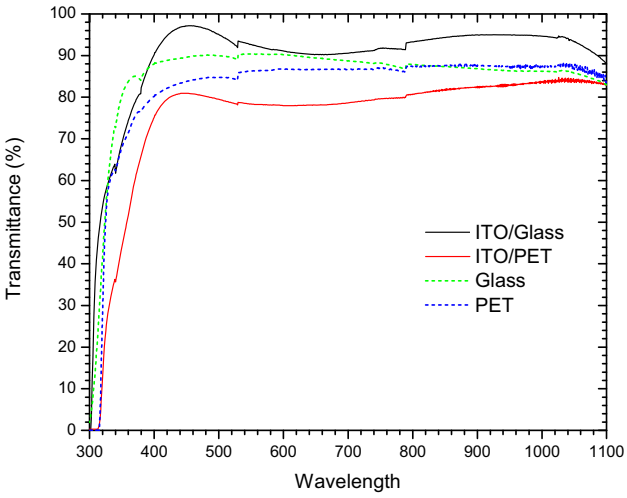

Figure 1: The transmittance of ITO on glass and PET substrates (solid), and the transmittance of the glass and PET substrates (dash line).

3.1 ITO removal by 266 nm, ns laser

The penetration depth of a laser pulse onto materials depends on the laser parameters as well as the material properties. The absorption coefficient, α_t of ITO, is $3.9 \times 10^7\ m^{-1}$ [24], while the thermal diffusion length can be estimated from $L = (2D\tau)^{1/2}$, where, D = thermal diffusivity of ITO ($4.5 \times 10^{-6}\ m^2s^{-1}$) [36] and τ = pulse length of the laser (8 ns). Thus, the thermal diffusion length is estimated to be ~268 nm, which is higher than the optical penetration depth of 25 nm. Thus, the removal process of ITO by the 266 nm ns laser is expected to be dominated by thermal process. In addition, laser-induced heat is transferred to the substrate beyond the thickness of the ITO layer.

Figure 2 shows the size of the ablation spot by a single laser pulse at different laser energies. The optical microscope images of the sample are also shown; the bright/white area is the area where ITO is removed, while ITO is damaged at the darkened area. For ITO on PET, ITO layer is removed from PET substrates above 0.7 mJ. At 2.2 mJ, the center of the ablation spot appeared damaged instead of being removed. For ITO on glass substrate, no removal is observed within the same laser energy range. At 3 mJ, a damaged area in the ablation spot is also observed. The darkening of ITO on glass caused by single laser pulse has also been reported when a ns laser is at 1,064 nm above $3\ J/cm^2$ [37]. Based on the results, we estimate the threshold for (i) removal of ITO from PET, (ii) modification of ITO on PET, and (iii) modification of ITO on glass from the plot of diameter^2 versus laser

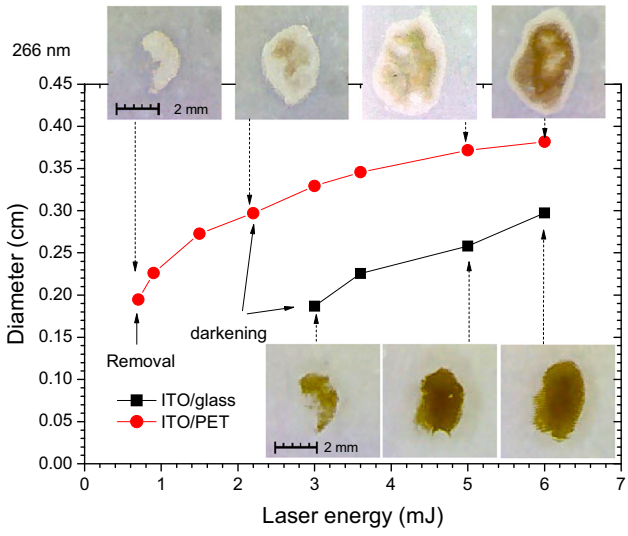

Figure 2: The diameter of the ablated area at different laser energies for ITO/glass and ITO/PET by 266 nm, ns laser.

fluence according to Liu's method [38] in Figure 3. In the method, the spatial distribution of the fluence is given by:

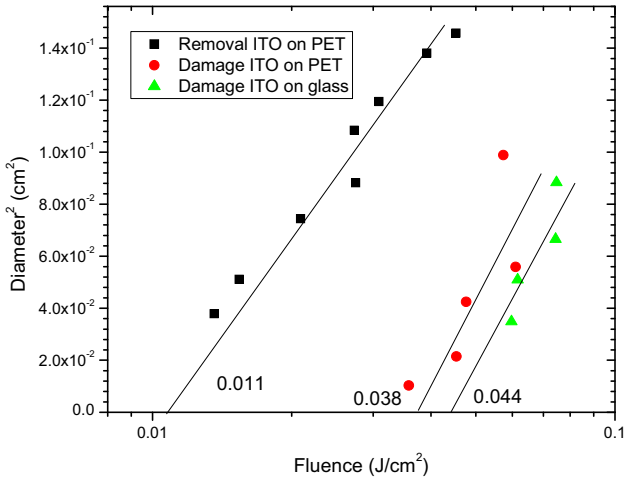

Figure 3: The threshold fluence for ITO on glass and ITO on PET by 266 nm, ns laser.

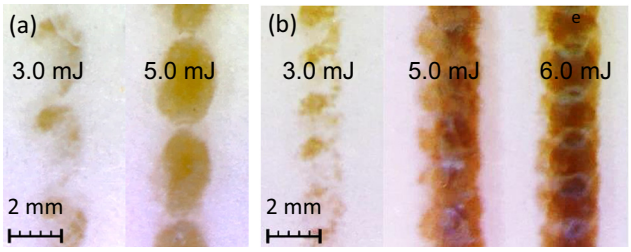

Figure 5: Ablation spots of ITO on glass with different laser energies (a) scanned at 1,000 mm/min and (b) scanned at 500 mm/min.

$$\phi_r = \phi_0 e^{\frac{-2r^2}{\omega_0^2}}$$

where ϕ_r is the fluence for the area with radius r, ϖ_0 is the $1/e^2$ beam radius, and ϕ_0 is the peak fluence. Thus, the equation becomes, $D^2 = 2\omega_0^2 \ln\left(\frac{\phi_0}{\phi_{th}}\right)$, where D is the diameter of the area of interest and the threshold fluence can be obtained when $D^2 = 0$. The threshold laser fluence for removal is 0.011 J/cm^2, while the threshold laser fluence for the damage of ITO on PET and on glass are similar (0.038, 0.044 J/cm^2). The damage threshold is significantly lower than that obtained using 1,064 nm [37] because of higher ITO absorption at 266 nm.

When the laser beam is scanned at different speed, overlapping of the ablation spot for ITO on PET (Figure 4) and glass (Figure 5) is obtained. For ITO on PET, the darken area is removed at the overlapping area of laser spots, as indicated by the arrow in Figure 4(a). The effect becomes significant as the scanning speed decreases (overlapping increases), the darken area is completely removed (Figure 4(b)), and electrical isolation is obtained across the patterned line.

For ITO on glass, darkened spots are obtained at a scan speed of 1,000 mm/min, while a continuous darken line is created as the overlapping increased at lower scan speed (Figure 5). The line, however, did not isolate the electrical path across. The sample is still conducting at the darken line and the measured resistance across the lines increases by 8× as compared to the unablated area. More intense damage is also observed at the overlapped

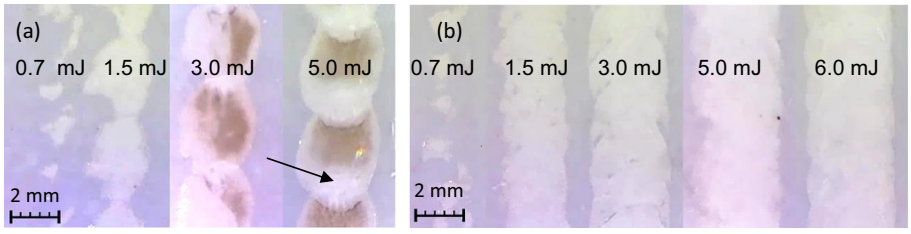

Figure 4: Ablation area of ITO on PET at different laser energies, (a) scanned at 1,000 mm/min and (b) scanned at 500 mm/min.

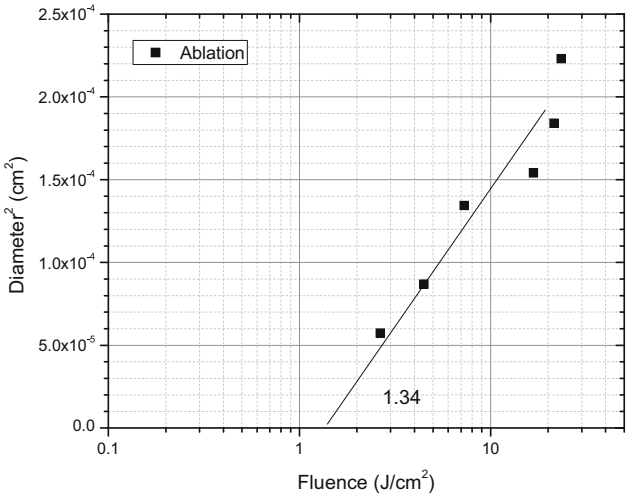

Figure 6: The threshold laser fluence for removal of ITO from glass by 266 nm, ns laser.

area of the laser pulse, due to the incubation effects of multiple pulses onto the same area. In order to obtain ITO removal on glass substrate, the laser beam spot is reduced and the laser fluence is increased (Figure 6). The threshold fluence for ITO removal is determined to be ~1.34 J/cm^2

3.2 ITO removal by 1,024 nm, fs laser

While fs laser interaction with transparent materials with wide bandgap (E_g), nonlinear processes are involved for modification and ablation [19]. Such interactions occur for ITO (E_g = 3.5–4.3 eV), PET (E_g = 3–4 eV) [39] as well as glass (E_g = 4–5 eV)[19] at high laser power with multi-photon absorption. The nonlinear refractive index (n_2) of ITO is 500 and the nonlinear absorption coefficient is −3 cm/GW [6]. For PET, n_2 is 13.1 [40], and for glass (BK7), n_2 is 2.23 and the nonlinear absorption coefficient is 2×10^{-4} cm/GW at 1,030 nm [41]. Thus, it is expected that the nonlinear absorption occurs readily in ITO, at low level in PET, and at the lowest level in glass.

The removal spots for ITO on PET by fs laser pulse at different laser fluence are shown in Figure 7. At 85 µJ, a small spot with diameter of ~50 µm is removed and some small fragments are also detected. As the laser energy is increased, the removed spot is larger and the maximum diameter is reached at 388 µJ. However, at 250 µJ, the center region is also damaged. The trend followed the Gaussian profile of the laser pulse where the center region is highest in fluence. The threshold laser fluences for the ablation and damage are determined from the diameter square versus fluence plot (Figure 8(a)). The AFM images of an unmodified PET surface and damaged area of PET are shown in Figure 8(b) and (c). The average roughness of the unmodified PET surface is only 1.1 nm, but the roughness of the modified/damaged area at the center is 12 nm. The corresponding threshold for removal of ITO on PET is 0.3 J/cm^2 and the substrate damage threshold is 0.8 J/cm^2.

For ITO on glass, single fs laser pulse at the same energy range as ITO/PET sample is not able to fully remove the ITO layer (Figure 9). The color contour corresponds to the different thicknesses of the ITO. When multiple laser pulse is used to obtain an isolated line, the

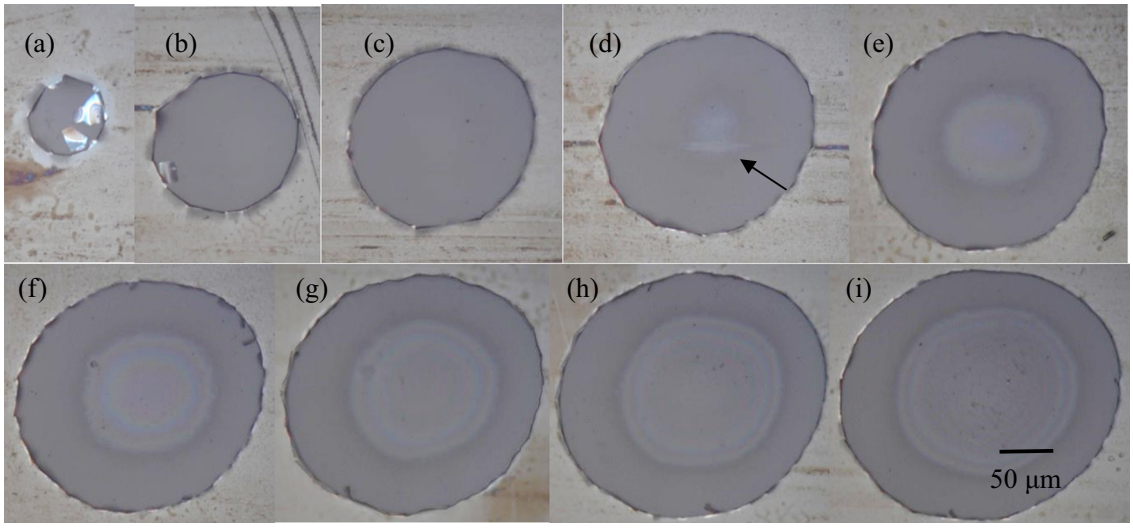

Figure 7: Fs laser removal of ITO on PET from 85 to 608 µJ. The central region is modified at 250 µJ and above (indicated by the arrow). (a) 85 µJ, (b) 134 µJ, (c) 184 µJ, (d) 250 µJ, (e) 317 µJ, (f) 388 µJ, (g) 458 µJ, (h) 521 µJ, (i) 608 µJ.

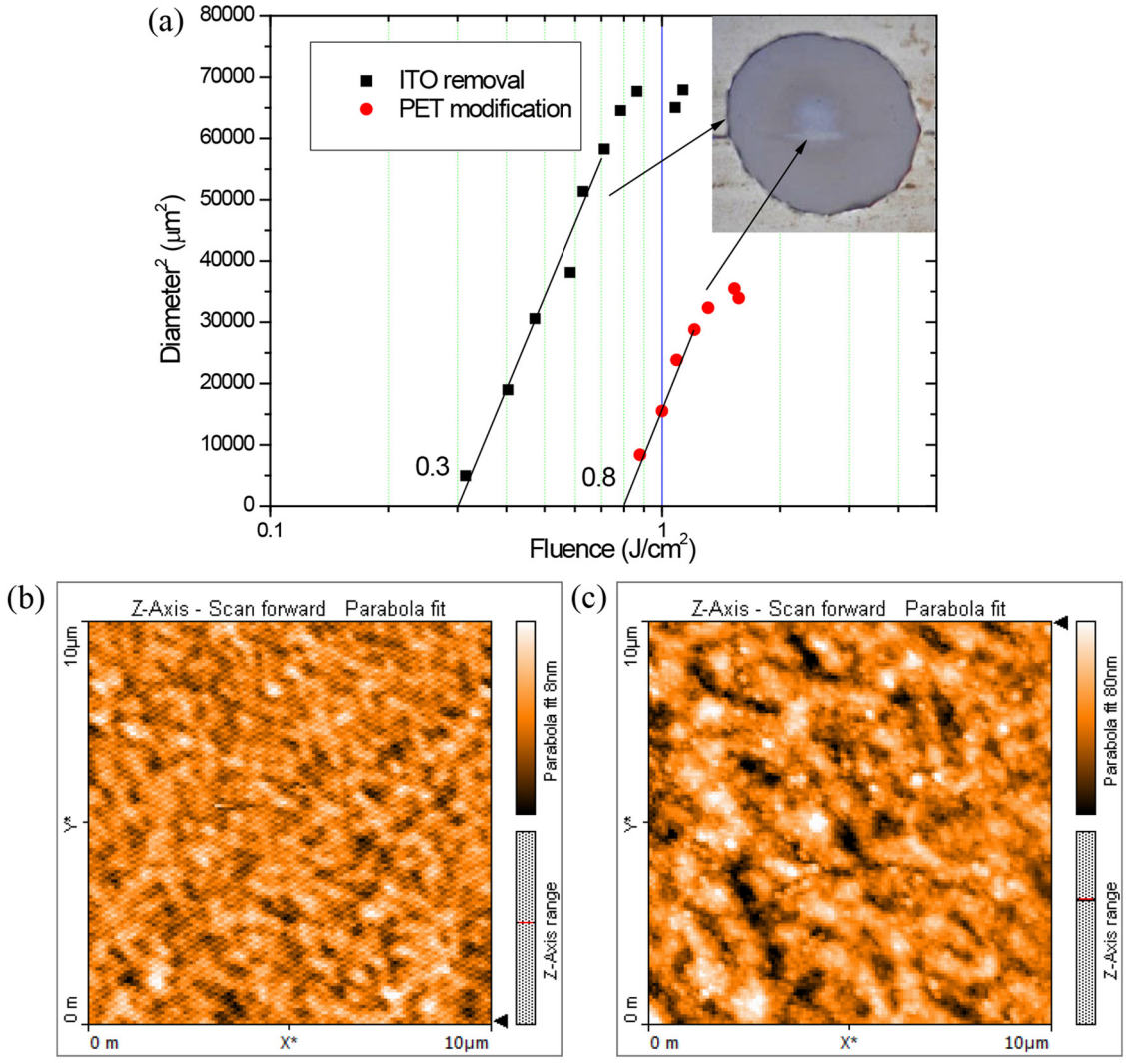

Figure 8: (a) Threshold fluence for fs laser ablation of ITO on PET (b) AFM images of the unmodified PET surface (left, color scale: 8 nm) with R_a = 1.1 nm and the modified PET surface at 250 μJ (right, color scale: 80 nm) where R_a = 12 nm, >10× higher than the unmodified PET surface.

generated lines are still conducting in Figure 9(a) and (b). The ITO layer on glass is only partially removed at lower fluence. Laser fluence of close to 1 J/cm^2 (Figure 9(d)) is needed to remove ITO with multiple pulses, and the area with fluence close to 0.3 J/cm^2 (the edge of the beam) is insufficient even with multiple pulses.

The laser fluence is increased by reducing the laser beam size and the ablated spots are shown in Figure 10. The removed area at the center of the laser-irradiated spot increases as the laser energy increases because of the Gaussian profile of the laser beam. The edge of the ablation spot is not as sharp as those obtained for ITO on PET as shown by the colored rings. Different degrees of ablation occurred as indicated by the color rings. Ablation that fully removed the ITO layer occurred only at the center region of the spot where the fluence is the highest. Based on the color contours, three main regions are defined. The outermost ring indicates the minimal ablation (region A) and the center region indicates full ITO removal (region C). There is an intermediate region where the fluence is just below that of the fluence required for full removal (region B). The 3D morphology and cross section of the ablated spot are shown in Figure 11(a) and (b). The corresponding ablated depths are 37 nm for region A, 78 nm for region B, and 109 nm for region C. From the plot of diameter^2 versus fluence, the threshold fluence is estimated to be 0.3 J/cm^2 for region A, 1.2 J/cm^2 for region B, and 1.7 J/cm^2 for region from Figure 11(c).

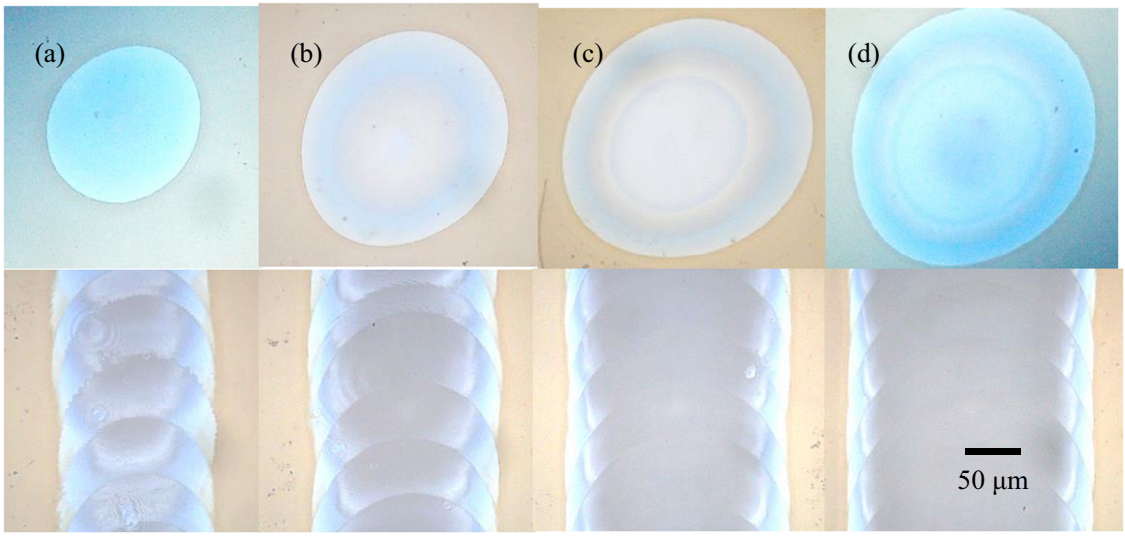

Figure 9: Single fs laser pulse is only able to partially remove the ITO layer on glass (top). Upon multiple laser pulses, some overlapped areas are fully removed (grey) at the corresponding laser energies (bottom). (a) 190 µJ, (b) 250 µJ, (c) 400 µJ, (d) 620 µJ.

3.3 Discussion

It is useful to determine the threshold fluence for ablation and the threshold for full removal of ITO by a single laser pulse. The threshold for ablation indicates the energy density at the onset for materials' removal based on laser-materials interaction, while the threshold for removal refers to the energy density required to fully remove the ITO layer (110–120 nm) in this work. The latter is beneficial for patterning of both electronics and photonics devices. It is also important to ensure that the patterning process does not induce any damage to the substrates. It is noted that ITO on PET samples is generally deposited at lower temperature than the ITO on glass. There is a slight variation in the properties of ITO and it is also expected that the adherence of ITO on the two types of substrate differs. Nevertheless, the process involved can be compared and discussed as summarized in Tables 1 and 2.

For 266 nm laser removal of ITO on PET, the threshold for removal is 100 times lower than ITO on glass. The large difference could be contributed by the thermomechanical properties of the substrates [28,34] and the lower adherence

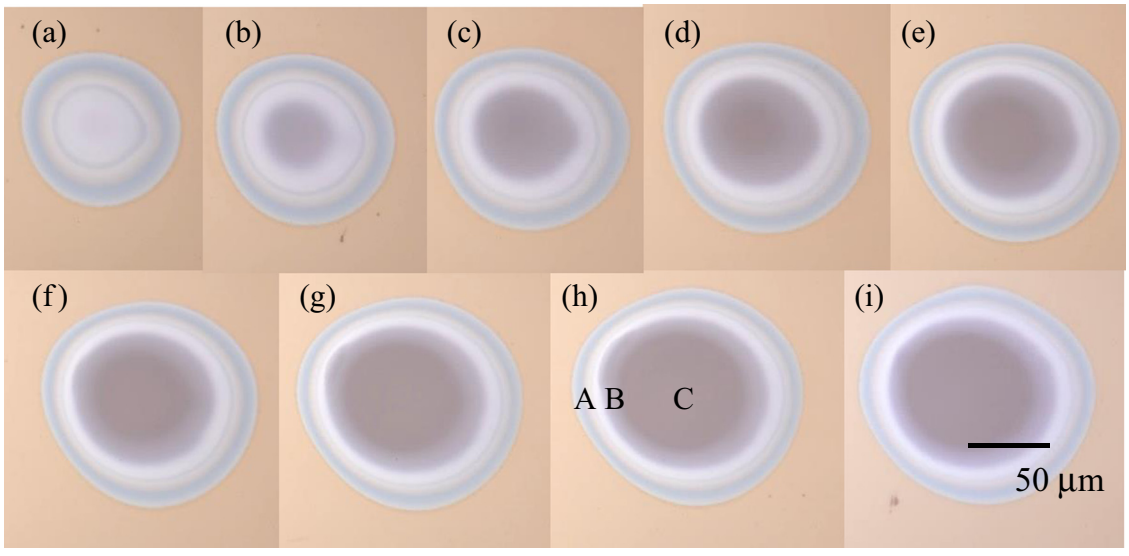

Figure 10: Fs laser removal of ITO on glass from 90 to 620 µJ. Different degrees of modification/ablation occurred because of the Gaussian profile of the laser beam. (a) 90 µJ, (b) 130 µJ, (c) 180 µJ, (d) 240 µJ, (e) 310 µJ, (f) 380 µJ, (g) 500 µJ, (h) 590 µJ, (i) 620 µJ.

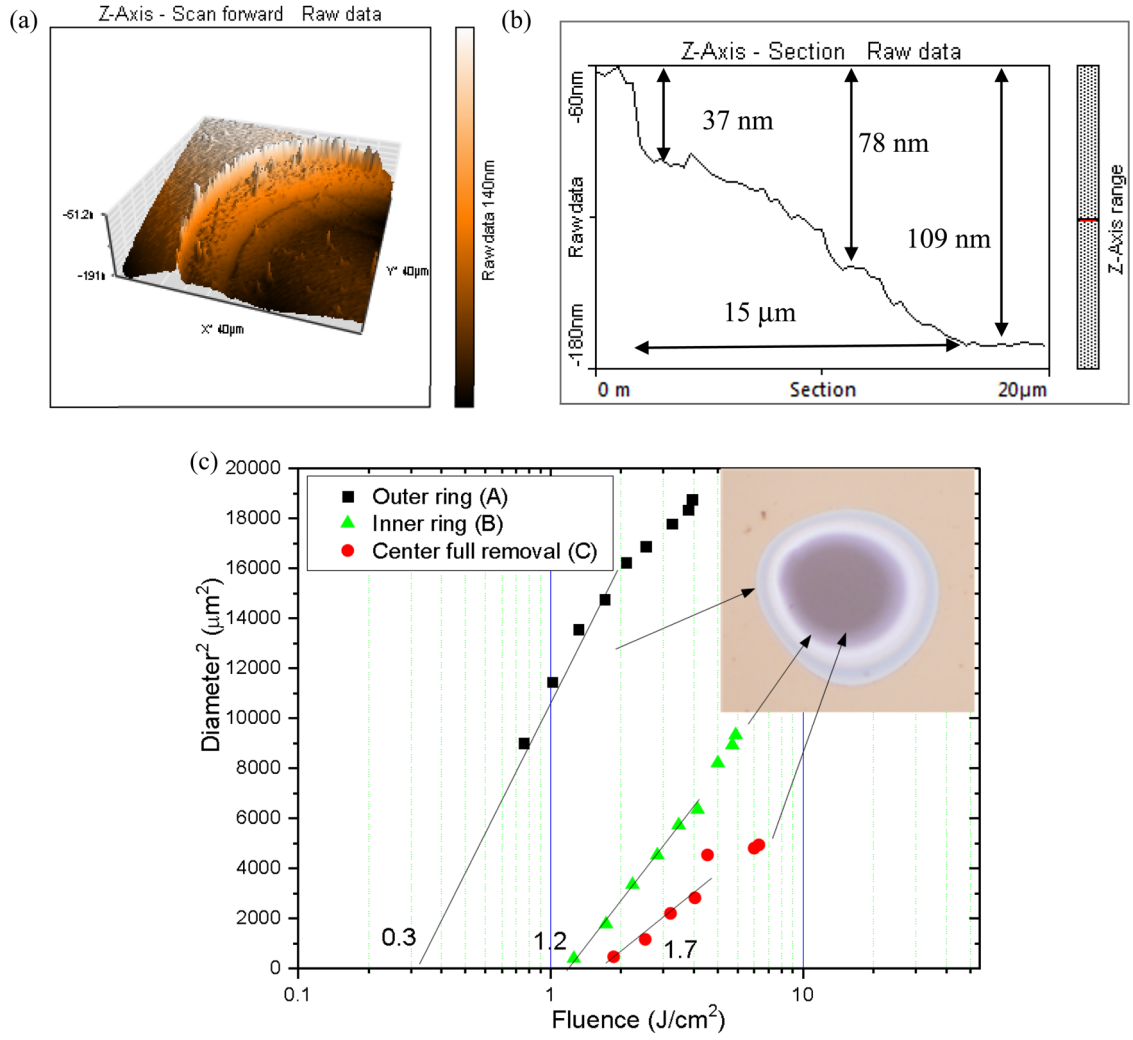

Figure 11: (a) The 3D contour of the ablation area obtained by AFM. (b) The cross section of the ablated spot. (c) The threshold fluence for 3 types of modifications by fs laser pulse on ITO/glass are determined from the diameter square versus fluence plot.

Table 1: Threshold fluence for ns laser interaction with ITO/PET and ITO/glass

266 nm 6 ns	Process	Threshold fluence (J/cm^2)	Remarks
ITO/PET	ITO removal	0.01	High absorption by ITO and PET, heat diffused to surrounding area. ITO removed via delamination
	ITO damage	0.038	High absorption by ITO, ITO damage at darken area
	PET modification	—	—
ITO/glass	ITO damage	0.044	High absorption by ITO, ITO damage at darken area
	ITO removal	1.34	ITO ablation with heat diffusion to surrounding area
	Glass modification	—	—

to PET. The ITO layer is removed easily from the PET substrate at threshold fluence below the threshold of ITO damage. The thermal conductivity of PET is ~10 times lower (0.14–0.4 W/mK) than BK7 glass (1.7 W/mK) [36]. In addition, PET can expand/deform when heated with thermal expansion coefficient of 20–80 ppm/K as compared to glass (8.3 ppm/K) and ITO (6.7 ppm/K) [36]. Thus, the large mismatch between ITO and PET likely contributes to the easy detachment of ITO from PET upon 266 nm laser irradiation [34].

ITO is highly absorptive at 266 nm and modification of ITO occurred at ~0.038–0.044 J/cm^2 for both substrates.

Table 2: Threshold fluence for fs laser interaction with ITO/PET and ITO/glass

1,025 nm 500 fs	Process	Threshold fluence (J/cm^2)	Process
ITO/PET	ITO removal	0.3	Nonlinear absorption with low heat diffusion ITO ablation + delamination
	PET modification	0.8	Nonlinear absorption effect on PET Ablation/modification of PET by residue laser pulse
ITO/glass	ITO partial removal	0.3	Nonlinear absorption with low heat diffusion, onset of ITO ablation
	ITO removal	1.7	Nonlinear absorption with low heat diffusion, full ITO removal
	Glass modification	—	—

Modified/damaged ITO regions are darkened and exhibited lower conductivity. For ITO on PET, the laser fluence required for the ITO damage is higher than that required for detachment from the PET substrates. On the other hand, for glass substrate, the threshold laser fluence for modification is lower than that of removal threshold. Thus, ITO is damaged at lower fluence before ablated at higher fluence. The darkening of ITO film has also been reported upon laser irradiation by 1,064 nm laser where the threshold laser fluence for damage was 100 times higher than the results obtained in this work [37]. Such a large difference is due to the high absorption coefficient of ITO at 266 nm (2,12,950/cm) as compared to 1625.9/cm at 1,000 nm.

In fs laser processing, no darkening was observed as in ns laser processing, suggesting that direct ablation occurred. For removal of ITO on PET, very clean removal can be achieved with a single laser pulse. Thermal processes are minimal as the laser pulse is short. Deformation due to the absorption of laser energy by the PET substrate is also minimal for fs laser irradiation. As a result, the threshold of 0.3 J/cm^2 is significantly higher (~30×) than those obtained by 266 nm laser. The threshold fluence for ITO/PET also coincides to the damage threshold of ITO on glass. Near the threshold, however, ITO fragments are also detected. The results indicate that the full removal from PET is to be dominated by ablation process, but stress release delamination may be coexisted near the threshold fluence [13]. In addition, our results show that the substrates are modified by the fs laser pulse beyond 0.8 J/cm^2. Bulk modification in transparent materials is achieved only by ultrafast laser when the intensity in the focal volume becomes high enough to induce permanent structural modifications and also a refractive index change or the formation of a small vacancy [42]. In our work, the change is caused by the residue energy that has transmitted through the ablated ITO layer, which is about ~0.5 J/cm^2.

The threshold fluence for ablation of ITO from glass substrate is 0.3 J/cm^2, but full removal of ITO by a single laser pulse only occurs at 1.7 J/cm^2. At ablation threshold of 0.3 J/cm^2, ITO layer with a thickness of 38 nm is removed. The ablation threshold obtained is comparable to other reports where thin ITO was used. The ablation threshold of fs laser were 0.30–0.45 J/cm^2 when laser pulse width of 60 to 600 fs were used [43]. In another work, the threshold of ablation (and removal) of 20 nm-thick ITO was 0.32 J/cm^2, obtained with the same laser wavelength and pulse width [26]. In the reports, in order to obtain full removal of thicker ITO, multiple pulses were required. Partial removal by a quasi-flat top beam was obtained by 1,030 nm, 190 fs laser at 0.8 and 0.9 J/cm^2, while complete removal is only obtained with 6 pulses [31,44]. Multiple overlapping ps laser pulses have led to depth control of 20 nm resolution [28]. When a 810 nm, 150 fs laser is used, the onset of ablation was estimated to be 0.07 J/cm^2 for 1TO (200 nm); single laser pulse was not able to fully remove the ITO[30]. In the current work, the single pulse removal threshold of 120 nm thick ITO is determined to be 1.7 J/cm^2 without substrate damage. The full removal threshold fluence is close to the fluence (1.5 J/cm^2) required to remove ~200 nm of 600 nm-thick ITO by a 300 fs, 1,030 nm laser [45]. The results suggest that ablation is to occur because of high nonlinear absorption of ITO. In addition, the laser fluence used in the current work is lower than single pulse laser damage threshold of glass in various report; namely, 2.9–3.6 J/cm^2 by 500 fs, 1,030 nm [46], 5.6 J/cm^2 by 150 fs, 800 nm laser [47], and >4 J/cm^2 by a 190 fs laser [48], which cause physical modification to the glass substrate. Thus, the fluence range for single pulse laser removal of ITO from glass without glass damage is proposed to be 1.7–2.9 J/cm^2.

4 Conclusion

The single pulse laser interaction with ITO is not only fundamentally important, but also potentially useful in microprocessing of various electronics and photonics devices. In this work, four different scenarios that

involved linear and nonlinear absorption process in ns and fs laser removal of ITO on PET or glass are investigated. The results show that ITO removal from PET can be easily achieved by using the 266 nm, ns laser (0.01 J/cm^2) because of the high linear absorption of the ns laser pulse and the thermomechanical properties of PET substrates. The high linear absorption of ITO in wavelength also results in ITO damage before the threshold fluence for ablation from glass substrate (1.34 J/cm^2). On the other hand, in nonlinear processes with a 1,025 nm, fs laser, direct ablation of ITO occurred on PET and glass substrate. Based on the differences in the characteristics of the ablation area, it is suggested that both ablation and stress release occurred for ITO/PET, while ablation occurred for ITO/glass in the studied fluence range. Fs laser processing also potentially induced unwanted damage to the transparent substrates. The fluence windows for removal are identified to be 0.3–0.8 J/cm^2 for ITO/PET and 1.7–2.9 J/cm^2.

Acknowledgments: The authors acknowledge the support from Sandisk/Western Digital Malaysia and the Ministry of Education, Malaysia (FRGS/1/2019/STG07/MMU/02/1).

Conflict of interest: The authors declare no conflict of interest regarding the publication of this paper.

References

[1] Betz U, Kharrazi Olsson M, Marthy J, Escolá MF, Atamny F. Thin films engineering of indium tin oxide: large area flat panel displays application. Surf Coat Technol. 2006;200:5751–9.
[2] Afre RA, Sharma N, Sharon M, Sharon M. Transparent conducting oxide films for various applications: a review. Rev Adv Mater Sci. 2018;53:79–89.
[3] Zhu R, Zhang Z, Li Y. Advanced materials for flexible solar cell applications. Nanotechnol Rev. 2019;8:452–8.
[4] Wei ZM, Xia JB. Recent progress in polarization-sensitive photodetectors based on low-dimensional semiconductors. Nanotechnol Rev. 2018;7:393–411.
[5] Ferrera M, Carnemolla EG. Ultra-fast transient plasmonics using transparent conductive oxides. J Opt (UK). 2018;20:024007.
[6] Alam MZ, De Leon I, Boyd RW. Large optical nonlinearity of indium tin oxide in its epsilon-near-zero region. Science. 2016;352:795–7.
[7] Reshef O, De Leon I, Alam MZ, Boyd RW. Nonlinear optical effects in epsilon-near-zero media. Nat Rev Mater. 2019;4:535–51.
[8] Malureanu R, Lavrinenko A. Ultra-thin films for plasmonics: a technology overview. Nanotechnol Rev. 2015;4:259–75.
[9] Fang X, Mak CL, Zhang S, Wang Z, Yuan W. Pulsed laser deposited indium tin oxides as alternatives to noble metals in the near-infrared region. J Phys Condens Matter. 2016;28:224009.
[10] Yavas O, Takai M. High-speed maskless laser patterning of indium tin oxide thin films. Appl Phys Lett. 1998;83:2558.
[11] Tseng SF, Hsiao WT, Huang KC, Chiang D, Chen MF, Chou CP. Laser scribing of indium tin oxide (ITO) thin films deposited on various substrates for touch panels. Appl Surf Sci. 2010;257:1487–94.
[12] Shin H, Sim B, Lee M. Laser-driven high-resolution patterning of indium tin oxide thin film for electronic device. Opt Laser Eng. 2010;48:816–20.
[13] Karnakis D, Kearsley A, Knowles M. Ultrafast laser patterning of OLEDs on flexible substrate for solid-state lighting. J Laser Micro Nanoeng. 2009;4:218–23.
[14] Chen MF, Chen YP, Hsiao WT, Gu ZP. Laser direct write patterning technique of indium tin oxide film. Thin Solid Films. 2007;515:8515–8.
[15] Chen MF, Hsiao WT, Ho YS, Tseng SF, Chen YP. Laser patterning with beam shaping on indium tin oxide thin films of glass/plastic substrate. Thin Solid Films. 2009;518:1072–8.
[16] Bäuerle D. Laser processing and chemistry (vol 4). Berlin: Springer-Verlag; 2011. p. 489–531.
[17] Rayner DM, Naumov A, Corkum PB. Ultrashort pulse non-linear optical absorption in transparent media. Opt Express. 2005;13:3208.
[18] Sugioka K, Cheng Y. Ultrafast lasers-reliable tools for advanced materials processing. Light Sci Appl. 2014;3:1–12.
[19] Gattass RR, Mazur E. Femtosecond laser micromachining in transparent materials. Nat Photon. 2008;2:219–25.
[20] Jiang LJ, Maruo S, Osellame R, Xiong W, Campbell JH, Lu YF. Femtosecond laser direct writing in transparent materials based on nonlinear absorption. MRS Bull. 2016;41:975–83.
[21] Cerkauskaite A, Drevinskas R, Solodar A, Abdulhalim I, Kazansky PG. Form-birefringence in ITO thin films engineered by ultrafast laser nanostructuring. ACS Photonics. 2017;4:2944–51.
[22] Yeung KW, Dong Y, Chen L, Tang CY, Law WC. Printability of photo – sensitive nanocomposites using two – photon polymerization. Nanotechnol Rev. 2020;9:418–26.
[23] Yavas O, Takai M. Effect of substrate absorption on the efficiency of laser patterning of indium tin oxide thin films. J Appl Phys. 1999;85:4207–12.
[24] McDonnell C, Milne D, Chan H, Rostohar D, O'Connor GM. Part 1: wavelength dependent nanosecond laser patterning of very thin indium tin oxide films on glass substrates. Opt Laser Eng. 2016;80:73–82.
[25] Račiukaitis G, Brikas M, Gedvilas M, Rakickas T. Patterning of indium-tin oxide on glass with picosecond lasers. Appl Surf Sci. 2007;253:6570–4.
[26] McDonnell C, Milne D, Chan H, Rostohar D, O'Connor GM. Part 2: ultra-short pulse laser patterning of very thin indium tin oxide on glass substrates. Opt Laser Eng. 2016;81:70–8.
[27] Choi HW, Farson DF, Bovatsek J, Arai A, Ashkenasi D. Direct-write patterning of indium-tin-oxide film by high pulse repetition frequency femtosecond laser ablation. Appl Opt. 2007;46:5792.
[28] Farid N, Chan H, Milne D, Brunton A, O'Connor GM. Stress assisted selective ablation of ITO thin film by picosecond laser. Appl Surf Sci. 2018;427:499–504.

[29] Kim J, Lee S, Bae JS, Park S, Choi U, Cho C. Electric properties and surface characterization of transparent Al-doped ZnO thin films prepared by pulsed laser deposition. Thin Solid Films. 2008;516:5223–6.
[30] Park M, Chon BH, Kim HS, Jeoung SC, Kim D, Lee JI, et al. Ultrafast laser ablation of indium tin oxide thin films for organic light-emitting diode application. Opt Laser Eng. 2006;44:138–46.
[31] Kim HY, Yoon JW, Choi WS, Kim KR, Cho SH. Ablation depth control with 40 nm resolution on ITO thin films using a square, flat top beam shaped femtosecond NIR laser. Opt Laser Eng. 2016;84:44–50.
[32] Haskal EI, French ID, Lifka H, Sanders R, Bouten P, Kretz T, et al. Flexible OLED displays made with the EPLaR process. SID conference record of the international display research conference; 2007.
[33] Zhang T, Liu D, Park HK, Yu DX, Hwang DJ. High resolution laser patterning of ITO on PET substrate. Proceedings SPIE 8607, laser applications in microelectronic and optoelectronic manufacturing (LAMOM) XVIII; 2013. p. 860712
[34] McDonnell C, Milne D, Prieto C, Chan H, Rostohar D, O'Connor GM. Laser patterning of very thin indium tin oxide thin films on PET substrates. Appl Surf Sci. 2015;359:567–75.
[35] Xiao S, Fernandes SA, Ostendorf A. Selective patterning of ITO on flexible PET Substrate by 1,064 nm picosecond Laser. Phys Procedia. 2011;2:125–32
[36] Yoo J-H, Matthews M, Ramsey P, Barrios AC, Carter A, Lange A, et al. Thermally ruggedized ITO transparent electrode films for high power optoelectronics. Opt Express. 2017;25:25533.
[37] Yoo J-H, Menor MG, Adams JJ, Raman RN, Lee JRI, Olson TY, et al. Laser damage mechanisms in conductive widegap semiconductor films. Opt Express. 2016;24:17616.
[38] Liu JM. Simple technique for measurements of pulsed Gaussian-beam spot sizes. Opt Lett. 1982;7:196.
[39] Chen L, Batra R, Ranganathan R, Sotzing G, Cao Y, Ramprasad R. Electronic structure of polymer dielectrics: the role of chemical and morphological complexity. Chem Mater. 2018;30:7699–706.
[40] Tamer I, Hornung M, Lukas L, Hellwing M, Keppler S, Van Hull R, et al. Characterization and application of nonlinear plastic materials for post-CPA pulse compression. Opt Lett. 2020;45:6575–8.
[41] Flom SR, Beadie G, Bayya SS, Shaw B, Auxier JM. Ultrafast Z-scan measurements of nonlinear optical constants of window materials at 772, 1030, and 1550 nm. Appl Opt. 2015;54:F123.
[42] Itoh K, Watanabe W, Nolte S, Schaffer CB. Ultrafast processes for bulk modification of transparent materials. MRS Bull. 2006;31:620–5.
[43] Bian Q, Yu X, Zhao B, Chang Z, Lei S. Femtosecond laser ablation of indium tin-oxide narrow grooves for thin film solar cells. Opt Laser Technol. 2013;45:395–401.
[44] Kim HY, Jeon JW, Choi W, Shin YG, Ji SY, Cho SH. Ridge minimization of ablated morphologies on ITO thin films using squared quasi-flat top beam. Materials. 2018;11:1–10.
[45] Krause S, Miclea PT, Steudel F, Schweizer S, Seifert G. Precise microstructuring of indium-tin oxide thin films on glass by selective femtosecond laser ablation. EPJ Photovolt. 2013;4:2–6.
[46] Nieto D, Arines J, O'Connor GM, Flores-Arias MT. Single-pulse laser ablation threshold of borosilicate, fused silica, sapphire, and soda-lime glass for pulse widths of 500 fs, 10 ps, 20 ns. Appl Opt. 2015;54:8596.
[47] Campbell S, Dear FC, Hand DP, Reid DT. Single-pulse femtosecond laser machining of glass. J Opt A Pure Appl Opt. 2005;7:162–8.
[48] Garcia-Lechuga M, Utéza O, Sanner N, Grojo D. Evidencing the nonlinearity independence of resolution in femtosecond laser ablation. Opt Lett. 2020;45:952.